Pergamon

J. Quant. Spectrosc. Radiat. Transfer Vol. 59, No. 3–5, pp. 495–509, 1998

Printed in Great Britain
PII: S0022-4073(97)00124-6
0022-4073/98 $19.00 + 0.00

IMPROVED SPECTRAL PARAMETERS FOR THE THREE MOST ABUNDANT ISOTOPOMERS OF THE OXYGEN MOLECULE

ROBERT R. GAMACHE,†‡ AARON GOLDMAN§ and LAURENCE S. ROTHMAN‖

†Department of Environmental, Earth, and Atmospheric Sciences, University of Massachusetts Lowell, 1 University Avenue, Lowell, MA 01854, U.S.A., §Department of Physics, University of Denver, Denver, CO 80208, U.S.A. and ‖AF Geophysics Directorate, 29 Randolph Road, Hanscom AFB, Hanscom, MA 01731, U.S.A.

Abstract—Line positions, intensities, transition-moment squared, and lower state energies are calculated for the three most abundant isotopomers of the oxygen molecule in the terrestrial atmosphere, $^{16}O_2$, $^{18}O^{16}O$, and $^{17}O^{16}O$. All lines passing a wavenumber dependent cutoff procedure (3.7×10^{-30} cm^{-1}/(molecule cm^{-2}) at 2000 cm^{-1}) are retained for the 1996 HITRAN database. Halfwidths as a function of the transition quantum numbers are determined from the available experimental measurements. Explicit expressions are obtained relating line intensities to the transition-moment squared, the vibrational band intensity, and the electronic-vibrational Einstein-A coefficient. The statistical degeneracy factors are presented and misuse of these factors in previous works is explained. Finally, band-by-band comparisons between the new calculations and the data from the previous HITRAN database are made.

1. INTRODUCTION

Atmospheric spectra of oxygen are used for deducing information about properties and other species in the atmosphere, for example, measurements of O_2 emission are used as a standard for O_3 profile analysis.[1,2] There is a need to have available the most accurate parameters for this molecule. The spectrum of the oxygen molecule, even though O_2 is a simple diatomic, is unexpectedly complex. The oxygen molecule has two unpaired electrons with a total spin of 1 in the electronic ground state. There are two low-lying excited electronic states which give rise to near-I.R. and visible spectra, and the symmetries of the isotopomers, $^{16}O_2$, $^{16}O^{18}O$, and $^{16}O^{17}O$, affect the number of allowed states. In addition, both magnetic dipole and electric quadrupole transitions occur, the degeneracy of states needs to be carefully considered, and transitions occur from the microwave to the visible. Although the line intensities are usually small, the high mixing ratio and long optical path in the terrestrial atmosphere compensate to produce meaningful absorption.[3]

In this work, the spectral parameters for the oxygen molecule are calculated for the electronic-vibrational bands listed in Table 1. These data represent an improvement to the data contained on the 1992 version of the HITRAN molecular absorption database,[4] which are from calculations made in 1982.[5] The calculations consider the lower state energy, the wavenumber of the transition, the line intensity, and transition moment squared of the spectral lines. In addition, halfwidths as a function of transition quantum number are determined from the available experimental measurements. All fundamental physical constants used in the calculations are those reported by Cohen and Taylor.[6] The calculations were made in double precision on several different computer systems using codes written in FORTRAN. Below, we discuss the theory of molecular oxygen and describe the improvements to the data for each band.

‡To whom all correspondence should be addressed.

Table 1. Electronic-vibrational bands of O_2 from 0 to 16,000 cm^{-1}

Electronic band	Isotopomer $^{16}O_2$ $v'\leftarrow v''$	$^{16}O^{18}O$ $v'\leftarrow v''$	$^{16}O^{17}O$ $v'\leftarrow v''$
$X^3\Sigma_g^-\leftarrow X^3\Sigma_g^-$	0←0	0←0	0←0
	1←0		
	1←1		
$a^1\Delta_g\leftarrow X^3\Sigma_g^-$	0←1	0←0	
	0←0		
	1←0		
$b^1\Sigma_g^+\leftarrow X^3\Sigma_g^-$	0←0	0←0	
	1←0	1←0	1←0
	2←0	2←0	
	1←1		
	0←1		

2. GENERAL THEORY

To understand the spectrum of the molecular oxygen in the atmosphere, one must consider the properties of the three most abundant isotopic species of oxygen and the structure of the three lowest-lying electronic states. An excellent review for this material can be found in Herzberg.[7,8]

The theoretical treatment of the ground state of molecular oxygen was first given by Tinkham and Strandberg[9] and it was later clarified with the aid of the transformation theory of spherical tensors by Steinbach and Gordy.[10,11] References 12 and 13 give excellent overviews of the theory. The ground electronic state of the oxygen molecule is the $X^3\Sigma_g^-$ state. There are also two low-lying electronic states, the $a^1\Delta_g$ state and the $b^1\Sigma_g^+$ state at 7918 cm^{-1} and 13 195 cm^{-1} above the ground state, respectively. Since the electronic ground state is the $X^3\Sigma_g^-$ state, the average electronic orbital angular momentum vanishes ($\Lambda = 0$). Still there is an instantaneous non-zero value of the orbital angular momentum which produces a precessing magnetic dipole moment of orbital origin. The total electronic spin is $S = 1$, so that molecular oxygen has a permanent magnetic dipole moment of approximately two Bohr magnetons. The energy is described in terms of the total electronic spin vector, **S**, and the rotational angular momentum, **N**. In the electronic ground state, Hund's coupling case (b) dominates[7] (more recent work shows the need for intermediate coupling) and the total angular momentum **J** is $\mathbf{J} = \mathbf{N} + \mathbf{S}$. Thus for each value of N there are 3 allowed values of J. The oxygen molecule can interact with an electromagnetic field via its magnetic dipole (md) moment or by its electric quadrupole (eq) moment. In this work, calculations are made for both md and eq lines of O_2.

The principal isotopic species, $^{16}O_2$, is unique in that it is the only homonuclear diatomic molecule of the three isotopomers on the database. Because of this symmetry and the fact that the oxygen-16 nuclei have zero nuclear spin, the molecule behaves as a Bose particle. Thus the total wavefunction must be symmetric with respect to inversion through the center. The spins of the individual electrons form a resultant $S = 1$ that gives rise to a coupling of electronic (S) and rotational angular momentum (N) yielding a triplet of states labeled by J; $J = N$, $J = N + 1$, and $J = N - 1$. The wavefunctions for the vibrational and nuclear motion are symmetric, whereas the electronic wavefunction for a Σ_g^- state is antisymmetric, indicating the only allowed rotational wave functions are those for odd (antisymmetric) N. The result is that half (all N even) of the states of $^{16}O_2$ are missing in the ground electronic state.

In the $a^1\Delta_g$ electronic state, the resultant of the individual electron spin is zero ($S = 0$) giving $J = N$, but the rotational levels are split into two, one symmetric (+) and one antisymmetric (−) state, by Λ-doubling. Because of the constraints placed on the wavefunction by Bose–Einstein statistics, only the (+) state is allowed and, although all N are occupied, only half the states are realized. The $b^1\Sigma_g^+$ electronic state also has $S = 0$ giving $N = J$ and the electronic wavefunction for the Σ_g^+ state is symmetric as are Ψ_{nuc} and Ψ_{vib}; thus the only rotational wavefunctions are the symmetric (N even) ones. Because of the symmetry of the $^{16}O_2$ species and the nuclear spin $I(^{16}O) = 0$, half of the rotational states of *each* electronic level are missing.

For the two isotopic species on the database, $^{16}O^{18}O$ and $^{16}O^{17}O$, inversion, through the center is no longer a valid symmetry operation. For this condition, all rotational levels of the molecule are allowed, both (+) and (−). The ground electronic state is a triplet, $J = N$ and $J = N \pm 1$,

with all N allowed, $N = 1, 2, 3, \ldots$. The two low-lying electronic states, $a^1\Delta_g$ and $b^1\Sigma_g^+$ are singlets ($J = N$) with all values of N (even and odd) starting at $N_{min} = \Lambda$. Note that for the $a^1\Delta_g$ state there is Λ-type doubling, thus each N has two states.

Figure 1 is a rotational state diagram for the lowest three electronic states of O_2. A note of caution here: the rotational states of a diatomic molecule are classified according to the behavior of the *total wavefunction* with respect to reflection at the origin and not of the rotational wavefunction alone (see pp. 128–129 of Ref. 7). Thus in the diagram, the states labeled (+) in the $X^3\Sigma_g^-$ state correspond to N = odd (antisymmetric) states; whereas the states labeled (+) in the $b^1\Sigma_g^+$ state correspond to N = even (symmetric) states. The principal species of oxygen, $^{16}O_2$, follows Bose–Einstein statistics and as such does not have any of the (−) symmetry levels. Thus in the diagram all (−) states are eliminated, in the $X^3\Sigma_g^-$ state all even N levels are missing, in the $a^1\Delta_g$ state one level for each N is missing, and in the $b^1\Sigma_g^+$ state all odd N are missing. For the non-homonuclear species all levels are allowed. These symmetry factors have an important role in the statistics of the molecular. Taking the ratio of the number of levels in the $X^3\Sigma_g^-$ state to the $a^1\Delta_g$ state gives 3:2 regardless of the isotopomer (this is because for $^{16}O_2$ half the levels are missing in each electronic state). Likewise the similar ratio of the $X^3\Sigma_g^-$ state to the $b^1\Sigma_g^+$ state is 3:1.

3. LINE INTENSITIES

Various formulas are used to calculate the line intensities depending on the particular transition. Below these formulas are presented along with other relationships needed for the calculations. Also presented are relationships to explain problems encountered in determining the Einstein-A coefficients for transitions in the $X^3\Sigma_g^- \rightarrow a^1\Delta_g$ band. The transitions involve, in general, different electronic, lambda doubling, vibrational, and rotational states which will be labeled by ε,Λ,v, and (J,M), respectively with the usual spectroscopic notation of a single prime for the upper state and a double prime for the lower state. In the absence of an electric or magnetic field, the M states are degenerate and will be summed over to express the line intensity for the transition labeled by $\varepsilon''\Lambda''v''J'' \rightarrow \varepsilon'\Lambda'v'J'$. In the following, a shorthand notation will be adopted by substituting η for

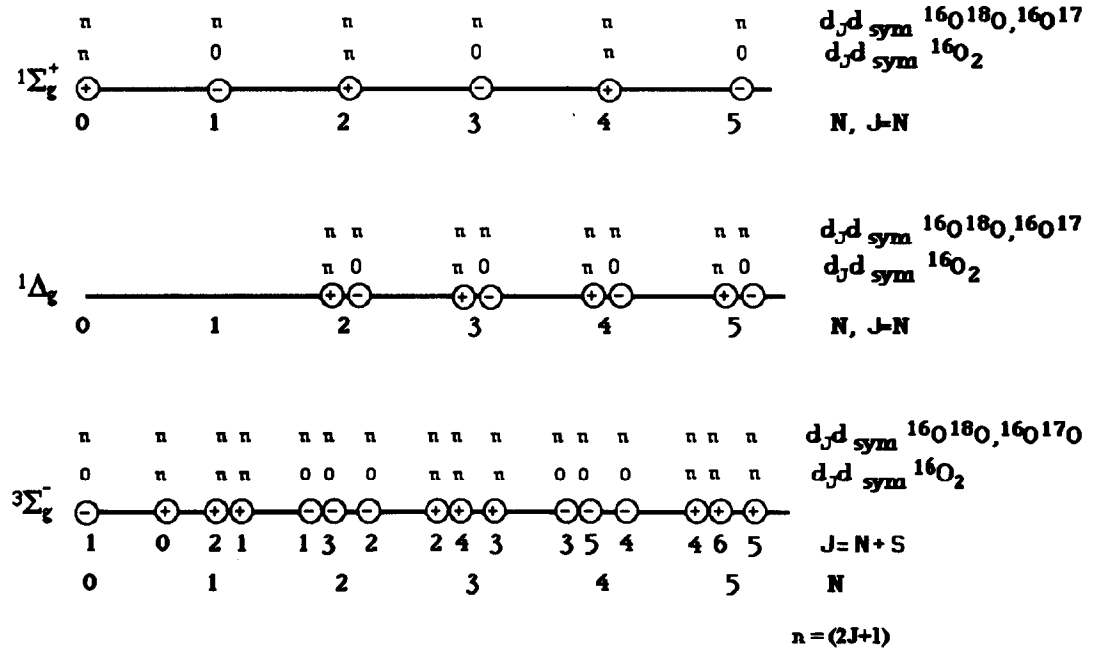

Fig. 1. State diagram for the three lowest electronic levels of the oxygen molecule, $X^3\Sigma_g^-$, $a^1\Delta_g$, and $b^1\Sigma_g^+$, and their statistical weights.

the set of quantum numbers $\varepsilon\Lambda vJ$. Thus $\eta'' \equiv \varepsilon''\Lambda''v''J''$ and $\eta' \equiv \varepsilon'\Lambda'v'J'$. The line intensity in units of (cm^{-1}/molecule cm^{-2}) for a transition $\eta'' \rightarrow \eta'$ is (see Refs. 14 and 15)

$$S_{\eta''\rightarrow\eta'} = \frac{8\pi^3}{3hc} I_a \frac{(d_{\eta''} e^{-E_{\eta''}/kT})}{d_{J''} Q(T)} \frac{\nu_{(\eta'')(\eta')}}{c} \left(1 - e^{-h\nu_{(\eta'')(\eta')}/kT}\right) \sum_{M'',M'} |R_{(\varepsilon''\Lambda''v''J''M'')(\varepsilon'\Lambda'v'J'M')}|^2 \, 10^{-36}, \tag{1}$$

where the total internal partition sum, $Q(T)$, is

$$Q(T) = \sum_{\varepsilon\Lambda vJ} d_\varepsilon d_\Lambda d_v d_J d_{sym} e^{-E_{\varepsilon\Lambda vJ}/kT}, \tag{2}$$

and I_a is the isotopic abundance of the species, the factor 10^{-36} is needed for the units chosen. $|R_{(\varepsilon''\Lambda''v''J''M'')(\varepsilon'\Lambda'v'J'M')}|^2$ is the transition-moment squared and has units of Debye^2/molecule, $d_{\eta''}$ is the degeneracy and $E_{\eta''}$ the energy of the state η'', $\nu_{(\eta'')(\eta')}/c = \omega_{(\eta'')(\eta')}$ is the wavenumber of the transition, and all other variables are the usual constants. (Note, in Eq. (1) and in a few expressions that follow we have not canceled some of the degeneracy factors in order to emphasize the fractional number of molecules in the state η'', $N_{\eta''}$.) In this paper we use the 'regular' matrix elements while in the Gamache and Rothman (1992) paper[15] we used the 'weighted' ones. The degeneracy factors are given by the product of the degeneracy factors for the quantized motions, $d_\eta = d_\varepsilon d_v d_J d_{sym}$ with $d_\varepsilon = (2S + 1)$, $d_\Lambda = (2 - \delta_{\Lambda,0})$, $d_v = 1$, $d_J = (2J + 1)$, and d_{sym} is one for the heteronuclear species and the (+) states of the homonuclear species and zero for the (−) states of the homonuclear species. This factor accounts for the symmetry restrictions for the homonuclear diatomics (note, this gives an overall factor of 1/2 in the partition sum).

This expression can be written in terms of the Einstein-A coefficient by making use of the relationship[14]

$$A_{\eta'\rightarrow\eta''} = \frac{64\pi^4 \, 10^{-36}}{3h} \omega^3_{(\eta'')(\eta')} \frac{1}{d_{J'}} \sum_{M'',M'} |R_{(\varepsilon''\Lambda''v''J''M'')(\varepsilon'\Lambda'v'J'M')}|^2, \tag{3}$$

whence the line intensity is

$$S_{\eta''\rightarrow\eta'} = \frac{I_a}{8\pi c} \frac{(d_{\eta''} e^{-E_{\eta''}/kT})}{Q(T)} \frac{1}{\omega^2_{(\eta'')(\eta')}} \left(1 - e^{-h\nu_{(\eta'')(\eta')}/kT}\right) \frac{d_{J'}}{d_{J''}} A_{\eta'\rightarrow\eta''}. \tag{4}$$

The Einstein-A coefficient is usually determined from a measurement of a vibrational band intensity, $S^{\varepsilon''\Lambda''v''}_{\varepsilon'\Lambda'v'}$ so it is useful to formulate Eq. (1) and Eq. (4) in terms of this quantity. The integrated intensity for an electronic-vibration–rotation band in units of cm^{-1}/(molecule cm^{-2}) is given by[14]

$$S^{\varepsilon''\Lambda''v''}_{\varepsilon'\Lambda'v'} = \frac{8\pi^3 \, 10^{-36}}{3hc} \omega_{\varepsilon''\Lambda''v'')(\varepsilon'\Lambda'v')} \frac{(d_{\varepsilon''\Lambda''v''} e^{-E_{\varepsilon''\Lambda''v''}/kT})}{Q_{\varepsilon\Lambda v}} |R_{(\varepsilon''\Lambda''v'')(\varepsilon'\Lambda'v')}|^2. \tag{5}$$

(Note, this is similar to α/N_L (Ref. 14, p. 153 with $\alpha = \Sigma_{J''J'} S_{\varepsilon''\Lambda''v''J''\rightarrow\varepsilon'\Lambda'v'J'}$) with the exception that the radiation field term, $(1 - e^{-h\nu_{(\eta'')(\eta')}/kT})$, is explicitly retained in the rotational part of the intensity formula. Thus our definition of $S^{\varepsilon''\Lambda''v''}_{\varepsilon'\Lambda'v'}$ does not contain the approximate factor $(1 - e^{-h\nu_{(\varepsilon''\Lambda''v'')(\varepsilon'\Lambda'v')}/kT})$.) To implement Eq. (5), the electronic-vibration and rotation parts are separated using the product approximation for the total partition sum and the transition-moment squared, and the assumption of additivity of energy

$$Q_{tot} = Q_{\varepsilon\Lambda v} \cdot Q_{rot}, \tag{6}$$

$$\sum_{M'',M'} |R_{(\eta'')(\eta')}|^2 = |R_{(\varepsilon''\Lambda''v'')(\varepsilon'\Lambda'v')}|^2 \cdot |R_{(J'')(J')}|^2,$$

$$E_{\eta''} = E_{\varepsilon''\Lambda''v''} + E_{J''}.$$

Inserting these into Eq. (1) and rearranging terms yields

$$S_{\eta''\to\eta'} = \frac{8\pi^3\, 10^{-36}}{3hc} \frac{(d_{\varepsilon''\Lambda''v''} e^{-E_{\varepsilon''\Lambda''v''}/kT})}{Q_{\varepsilon\Lambda v}} \omega_{(\varepsilon''\Lambda''v'')(\varepsilon'\Lambda'v')} |R_{(\varepsilon''\Lambda''v'')(\varepsilon'\Lambda'v')}|^2 \tag{7}$$

$$\times I_a \frac{(d_{J''} d_{sym} e^{-E_{J''}/kT})}{d_{J''} d_{sym} Q_{rot}} \frac{\omega_{(\eta'')(\eta')}}{\omega_{(\varepsilon''\Lambda''v'')(\varepsilon'\Lambda'v')}} \left(1 - e^{-hv_{(\eta'')(\eta')}/kT}\right) |R_{(J'')(J')}|^2.$$

The first part of this expression is simply the band intensity as defined in Eq. (5); thus the line intensity can be written

$$S_{\eta''\to\eta'} = S^{\varepsilon''\Lambda''v''}_{\varepsilon'\Lambda'v'} I_a \frac{(d_{J''} d_{sym} e^{-E_{J''}/kT})}{d_{J''} d_{sym} Q_{rot}} \frac{\omega_{(\eta'')(\eta')}}{\omega_{(\varepsilon''\Lambda''v'')(\varepsilon'\Lambda'v')}} \left(1 - e^{-hv_{(\eta'')(\eta')}/kT}\right) |R_{(J'')(J')}|^2. \tag{8}$$

In what follows we will need the relationships between the Einstein coefficients and the electronic-vibrational transition-moment squared. They are

$$B_{\varepsilon''\Lambda''v''\to\varepsilon'\Lambda'v'} = \frac{8\pi^3\, 10^{-36}}{3h^2} |R_{(\varepsilon''\Lambda''v'')(\varepsilon'\Lambda'v')}|^2, \tag{9a}$$

$$B_{\varepsilon'\Lambda'v'\to\varepsilon''\Lambda''v''} = \frac{8\pi^3\, 10^{-36}}{3h^2} \frac{d_{\varepsilon''\Lambda''v''}}{d_{\varepsilon'\Lambda'v'}} |R_{(\varepsilon''\Lambda''v'')(\varepsilon'\Lambda'v')}|^2, \tag{9b}$$

and

$$A_{\varepsilon'\Lambda'v'\to\varepsilon''\Lambda''v''} = \frac{64\pi^4\, 10^{-36}}{3h} \omega^3_{(\varepsilon'\Lambda'v')(\varepsilon''\Lambda''v'')} \frac{d_{\varepsilon''\Lambda''v''}}{d_{\varepsilon'\Lambda'v'}} |R_{(\varepsilon''\Lambda''v'')(\varepsilon'\Lambda'v')}|^2. \tag{9c}$$

Solving Eq. 9c for the transition-moment squared and inserting into Eq. (5) gives the result

$$S^{\varepsilon''\Lambda''v''}_{\varepsilon'\Lambda'v'} = \frac{1}{8\pi c} \frac{(d_{\varepsilon''\Lambda''v''} e^{-E_{\varepsilon''\Lambda''v''}/kT})}{Q_{\varepsilon\Lambda v} \omega^2_{(\varepsilon'\Lambda'v')(\varepsilon''\Lambda''v'')}} \frac{d_{\varepsilon'\Lambda'v'}}{d_{\varepsilon''\Lambda''v''}} A_{\varepsilon'\Lambda'v'\to\varepsilon''\Lambda''v''}. \tag{10}$$

This expression allows the Einstein-A coefficient to be determined by measuring the integrated band intensity. This relationship with Eq. (8) allows the $\varepsilon''\Lambda''v''J''\to\varepsilon'\Lambda'v'J'$ line intensity to be written in terms of the Einstein $A_{\varepsilon'\Lambda'v'\to\varepsilon''\Lambda''v''}$ coefficient

$$S_{\eta''\to\eta'} = \frac{I_a}{8\pi c} \frac{(d_{\varepsilon''\Lambda''v''J''} e^{-E_{\varepsilon''\Lambda''v''J''}/kT})}{d_{J''}\, Q_{tot}} \frac{\omega_{(\varepsilon''\Lambda''v''J'')(\varepsilon'\Lambda'v'J')}}{\omega^3_{(\varepsilon''\Lambda''v'')(\varepsilon'\Lambda'v')}} \tag{11}$$

$$\times (1 - e^{-hv_{(\eta'')(\eta')}/kT}) L_{J''} \frac{d_{\varepsilon'\Lambda'v'}}{d_{\varepsilon''\Lambda''v''}} A_{\varepsilon'\Lambda'v'\to\varepsilon''\Lambda''v''}$$

where the partition function and the energy are no longer approximated and the Hönl–London factor is inserted for the rotational transition-moment squared. Note that the degeneracy factors preceding the Einstein-A coefficient account for the number of J and M states in the upper and lower electronic-vibration states and the degeneracy factors with the partition function term are $d_{\varepsilon\Lambda vJ} = (2S + 1)(2 - \delta_{\Lambda,0})(d_{sym})(2J + 1)$. From the symmetry arguments presented above, it is clear that the ratio of the degeneracy factors, $d_{\varepsilon'\Lambda'v'}/d_{\varepsilon''\Lambda''v''}$, is 2/3 for $X^3\Sigma_g^- \to a^1\Delta_g$ transitions and 1/3 for the $X^3\Sigma_g^- \to b^1\Sigma_g^+$ transitions.

For several of the bands calculated, the program employs the Einstein-A coefficients in units of sec^{-1}. Often one must work from measured vibrational band intensities. In order to make use of these values, we must convert from vibrational band intensity to the Einstein-A coefficient. This relationship was presented in Eq. (10). However, quite often in the literature the vibrational band intensity is reported in units of $cm^{-1}\,km^{-1}\,atm^{-1}$ STP. The values must be converted to the

HITRAN units of $cm^{-1}/(molecule\ cm^{-2})$ to apply the equations presented here. This is accomplished by the relationship

$$S_v^v\left(\frac{cm^{-1}}{molecule\ cm^{-2}}\right) \times \frac{N_L}{p(atm)} \times 10^5 \frac{cm}{km} = S_v^v(cm^{-1}km^{-1}atm^{-1}STP) \tag{12}$$

where N_L is Loschmidt's number, the number of molecules per cubic centimeter of perfect gas at STP. Thus we have

$$S_v^v\left(\frac{cm^{-1}}{molecule\ cm^{-2}}\right) \times 2.6867 \times 10^{24} \frac{cm}{km} = S_v^v(cm^{-1}km^{-1}atm^{-1}STP)\,. \tag{13}$$

From Eq. (10), the Einstein-A coefficients used in the program have been updated using vibrational band intensities reported in the literature. The vibrational band intensities and Einstein-A coefficients used in the program are presented in Table 2 for the $b^1\Sigma_g^+ \leftarrow X^3\Sigma_g^-$ band.

The vibrational band centers are computed using the following expressions

$$G(v) = \omega_e(v + 1/2) - \omega_e x_e(v + 1/2)^2 + \omega_e y_e(v + 1/2)^3 - \omega_e z_e(v + 1/2)^4\,, \tag{14}$$

$$G(v') = \omega_e'(v' + 1/2) - \omega_e x_e'(v' + 1/2)^2 + \omega_e y_e'(v' + 1/2)^3 - \omega_e z_e'(v' + 1/2)^4\,, \tag{15}$$

and

$$\omega_0 = T_e + G(v') - G(v)\,. \tag{16}$$

The constants (T_e, ω_e, $\omega_e x_e$, $\omega_e y_e$, $\omega_e z_e$, ω_e', $\omega_e x_e'$, $\omega_e y_e'$, $\omega_e z_e'$) are taken from Krupenie[16] for both the $a^1\Delta_g^+$ and $b^1\Sigma_g^+$ electronic states.

The partition sums used in the program are those from the TIPS[17] (Total Internal Partition Sum) program. Before addition to the HITRAN database, the line intensities are filtered through a wavenumber dependent cutoff given by

$$S_{cut} = S_{\omega_c}\left(\frac{\omega}{\omega_c}\right)\left\{\frac{1 - e^{-h\nu/kT}}{1 + e^{-h\nu/kT}}\right\} \tag{17}$$

with $\omega_c = 2000\ cm^{-1}$ and $S_{\omega_c} = 3.7 \times 10^{-30} cm^{-1}/(molecule\ cm^{-2})$. All lines with an intensity less than the cutoff are not included in the database with the exceptions noted below.

4. HALFWIDTHS

Measurements of the halfwidths are available for several bands of the O_2 molecule. The data of Krupenie[16] are taken for the $X^3\Sigma_g^-$ pure rotation bands, the A-band data are from Ritter and Wilkerson[18], the B-band data from Giver et al[19] and the γ-band data are from Mélières *et al.*[20] The

Table 2. Vibrational band intensities and Einstein-A coefficients for the $b^1\Sigma_g^+ \leftarrow X^3\Sigma_g^-$ band of O_2

Band	$S_{v'}^{v}$,[a]	$S_{v'}^{v}$,[b]	A[c]	Ref.	A(ref.)[c]	A(O_2,CALC)[c]
A band	532.	1.98×10^{-22}	0.0770	46	0.077	0.077
(0–0)	582.	2.17×10^{-22}	0.084	48	0.084	NA
		2.28×10^{-22}	0.0887	18	0.0887	NA
B band	40.8	1.52×10^{-23}	0.00724	19	NG	0.00591*
(1–0)	38.8	1.44×10^{-23}	0.00689	48	0.0069	NA
γ band	1.52	5.66×10^{-25}	3.24×10^{-4}	47	NG	2.212^{-4}*
(2–0)	1.50	5.58×10^{-25}	3.19×10^{-4}	48	3.2×12^{-4}	NA
	1.26	4.71×10^{-25}	2.69×10^{-4}	20	NG	NA
(3–0)	0.0269	1.00×10^{-26}	6.73×10^{-6}	48	6.7×12^{-6}	NA
(1–1)	0.136	5.06×10^{-26}	0.0701	48	0.0704	0.0704
(0–1)	0.0114	4.24×10^{-27}	0.00467	48	0.0047	0.0047

[a]Units of $cm^{-1}\ km^{-1}\ atm^{-1}$ STP.
[b]Units of $cm^{-1}/(molecule\ cm^{-2})$.
[c]Units of $sec^{-1}/molecule$.
*Does not agree with literature value (see text).
NA not applicable.
NG not given.

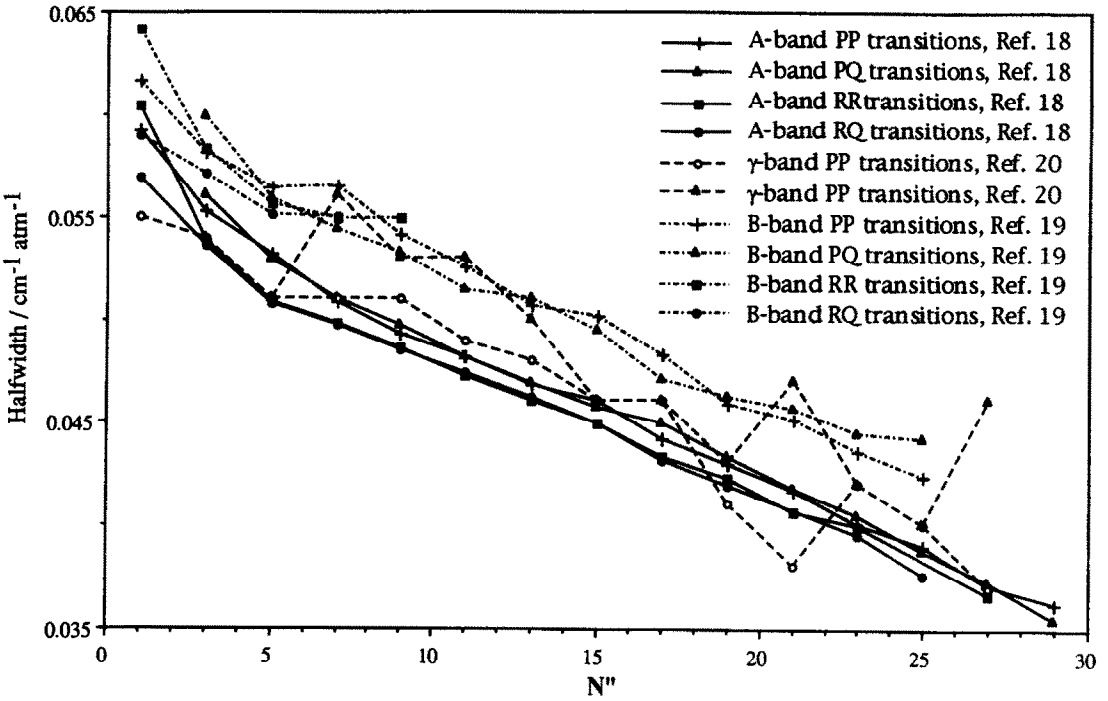

Fig. 2. Halfwidth data cm^{-1} atm^{-1} at 296 K for the A-, B- and γ bands of O_2 according to branches as a function of N.

data of Refs. 18–20 are plotted in Fig. 2 as a function of N'' for the various types of transitions. The transitions are labeled by $\Delta N \Delta J\, N''\, J''$; however with symmetry arguments the notation ${}^{\Delta N}\Delta J_{N''}$ is often used. For the A-band we find that if the ${}^{R}R$ and ${}^{R}Q$ values are shifted, $(N'' \rightarrow N'' + 2)$, they agree with the ${}^{P}P$ and ${}^{P}Q$ values (see Fig. 3), i.e.,

$$\gamma({}^{P}P_{N''}) = \gamma({}^{R}R_{N''+2})$$

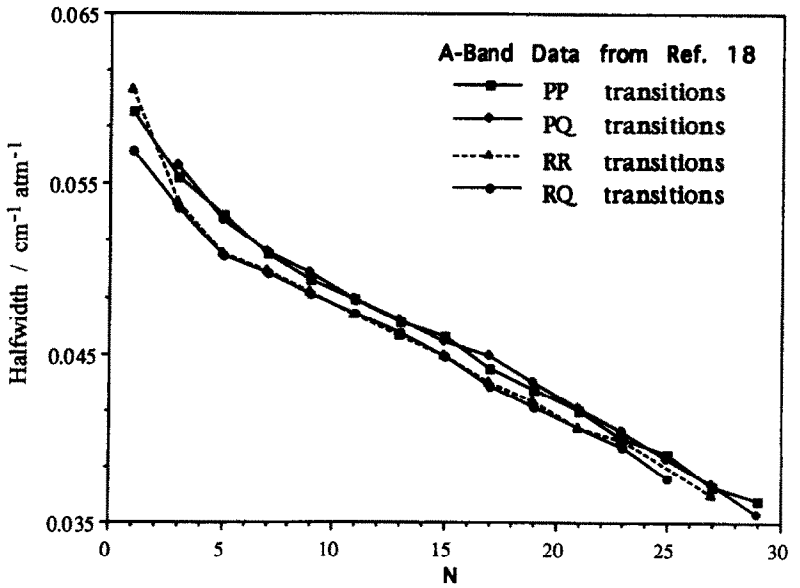

Fig. 3. A-band halfwidths cm^{-1} atm^{-1} at 296 K, RR and RQ values are shifted, $N'' \rightarrow N'' + 2$.

and

$$\gamma(^{P}Q_{N''}) = \gamma(^{R}Q_{N''+2}) \tag{18}$$

For the B-band, the difference between the ^{P}P, ^{P}Q, ^{R}R, and ^{R}Q values for a given N'' is small. The data of Mélières et al[20] for the γ-band, however, show large variations in the halfwidth as a function of N'' not seen in the other data (see open circles and triangles in Fig. 2).

Comparing the values from Refs. 18–20, we find that the A- and γ-band results agree with each other and the B-band results are some 10% larger. The data selected for O_2 on the 1996 HITRAN database use the following procedure for the halfwidths. The $X^3\Sigma_g^-$ pure rotation band uses the data reported by Krupenie[16] for the 60 GHz lines. The electric quadrupole transitions and the transitions involving the $a^1\Delta_g$ state use the A-band values.[18] For the A- and γ-bands, the halfwidths of Ritter and Wilkerson[18] are averaged as a function of N'' for the ^{P}P and ^{P}Q lines together and the ^{R}R and ^{R}Q lines together. We have calculated transitions to $N'' = 80$ and the measurements end at $N'' = 29$; thus it is necessary to extrapolate the data. From the plots, an asymptotic limit of $\gamma = 0.032$ cm^{-1}/atm for $N'' \geq 40$ is estimated. Both the R and P lines use the same asymptotic limit. The values of the halfwidths for the A- and B-bands of O_2 used in the HITRAN96 are given in Table 3.

5. UPDATES TO THE OXYGEN DATA FOR THE 1996 HITRAN DATABASE

Below, the changes made to the data for the 1996 HITRAN database are discussed for each band of molecular oxygen considered. The line position and energy differences are defined as the HITRAN92 value minus the HITRAN96 value. For the line intensities the ratio computed is HITRAN92/HITRAN96. The average and maximum differences were calculated for the line position and energy parameters. For the line intensities, the average, maximum and minimum ratios were calculated.

5.1. The principal isotopic species, $^{16}O_2$

5.1.1. The $X^3\Sigma_g^-$ ($v = 0$)← $X^3\Sigma_g^-$ ($v = 0$) band. The energy levels for the vibrational ground state of the $X^3\Sigma_g^-$ electronic state of $^{16}O_2$ are calculated using the formalism of Rouillé et al.[21] In this work the Hamiltonian included all rotational terms to second order[22] and some terms to third order.[23,24] The molecular constants are those of Rouillé et al.[21] These are compared with the energy values from the previous database (the energy levels for O_2 on the 1982–1992 versions of HITRAN

Table 3. Halfwidths in cm^{-1}/atm for the A- and B-bands of O_2

N''	A – P†	A – R‡	B§	N''	A – P†	A – R‡	B§
1	0.0592	0.0587	0.0616	21	0.0417	0.0406	0.0454
2	0.0574	0.0562	0.0600	22	0.0409	0.0402	0.0447
3	0.0557	0.0538	0.0584	23	0.0402	0.0397	0.0440
4	0.0544	0.0523	0.0571	24	0.0395	0.0386	0.0436
5	0.0531	0.0509	0.0558	25	0.0389	0.0376	0.0432
6	0.0520	0.0503	0.0555	26	0.0380	0.0371	0.0428
7	0.0509	0.0498	0.0552	27	0.0371	0.0366	0.0422
8	0.0502	0.0492	0.0547	28	0.0365	0.0183	0.0418
9	0.0495	0.0486	0.0541	29	0.0358	0.0358	0.0414
10	0.0488	0.0479	0.0531	30*	0.0353	0.0353	0.0410
11	0.0482	0.0473	0.0521	31*	0.0349	0.0349	0.0407
12	0.0475	0.0467	0.0515	32*	0.0345	0.0345	0.0404
13	0.0468	0.0461	0.0509	33*	0.0340	0.0340	0.0400
14	0.0464	0.0455	0.0504	34*	0.0337	0.0337	0.0398
15	0.0459	0.0449	0.0499	35*	0.0334	0.0334	0.0395
16	0.0452	0.0441	0.0488	36*	0.0330	0.0330	0.0394
17	0.0445	0.0432	0.0477	37*	0.0328	0.0328	0.0393
18	0.0438	0.0426	0.0469	38*	0.0324	0.0324	0.0391
19	0.0431	0.0421	0.0461	39*	0.0322	0.0322	0.0390
20	0.0424	0.0413	0.0457	40*	0.0320	0.0320	0.0390

†A-band ^{P}P and ^{P}Q transitions.
‡A-band ^{R}R and ^{R}Q transitions.
§B-band transitions.
*Extrapolated.

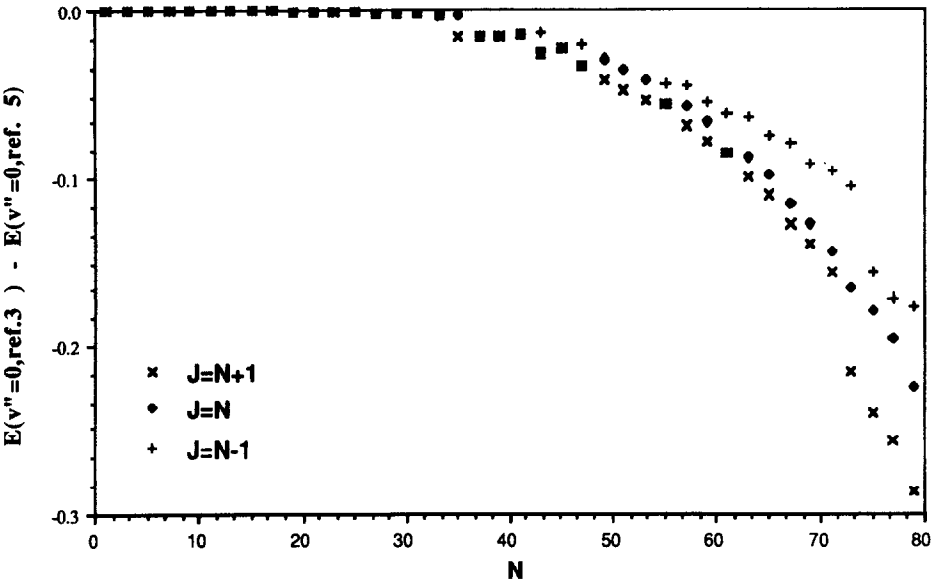

Fig. 4. Energy difference in cm^{-1} between the formalism of Rouillé et al[21] and Greenbaum[13] vs N for the $v'' = 0$ states of $X^3\Sigma_g^-$ of $^{16}O_2$.

used for the formulation of Ref. 13) in Fig. 4. The difference in energy between the two formulations is given as a function of N and J. For the vibrational ground state the difference is near zero for N up to 35, then rapidly goes to $-0.3\ cm^{-1}$ at $N = 80$. While the transition frequencies from this formulation differ only slightly from the previous results, $0.0039\ cm^{-1}$ maximum difference, $7 \times 10^{-5}\ cm^{-1}$ on average, the formalism of Rouillé et al[21] gives better agreement with measurements.‡

This band has both magnetic dipole and electric quadrupole transitions. For the electric quadrupole transitions, a newer value of the quadrupole moment derived from far-IR PIA spectra,[25] 0.34×10^{-26} esu cm^2, has been adopted. There are no data to validate the intensities we obtain. With this value for the quadrupole moment, the line intensities and transition-moments squared are a factor of 5.8 weaker than previous calculations.[26] Because of this reduction in the line intensities, no electric quadrupole lines survived the cutoff for the 1996 data set. This is further discussed below for the 1←0 vibrational band of this electronic band. The 1996 calculations of the magnetic dipole intensities are on average 4% stronger than the 1992 values. This is due to improved energy formulation and partition sums.

5.1.2. The $X^3\Sigma_g^-$ $(v = 1) \leftarrow$ $X^3\Sigma_g^-$ $(v = 0)$ *band.* The 1992 HITRAN database contained only electric quadrupole (eq) lines for this band. The newer data contain both magnetic dipole (md) and electric quadrupole (eq) transitions.[27] Thus, the comparison made here is for the electric quadrupole lines. The energy levels for the vibrational ground ($v = 0$) and the first fundamental ($v = 1$) of the $X^3\Sigma_g^-$ electronic state of $^{16}O_2$ are calculated using the formalism and constants of Rouillé et al.[21] These energies are compared with the values from the previous database[5] in Fig. 5 for the $v'' = 1$ states. The difference is small for N up to ≈ 20 then quickly goes to roughly $5\ cm^{-1}$ at $N = 80$. For the transitions that make the cutoff criterion, $N \leq 31$, the maximum difference in the energy values is $0.0024\ cm^{-1}$, $0.0005\ cm^{-1}$ on average. The corresponding average and maximum differences in the line positions are -0.0104 and $0.0850\ cm^{-1}$. The electric quadrupole transition line intensities are calculated using the formalism of Goldman et al.[27] The absolute intensities are determined by scaling the relative intensities to the measurements of Reid et al.[28] Comparison of these intensities with the 1992 HITRAN values implies an electric quadrupole moment of

‡Comparisons were made with the data from Refs. 20 and 32. The different formulations are compared with experiment for 30 lines measured in Ref. 32 and for 2 transitions measured in Ref. 20. The comparison shows the Rouillé et al formalism to be very slightly better than that of Ref. 13, with the average deviations being $0.00256\ cm^{-1}$ vs. $0.00259\ cm^{-1}$. respectively. Note the average deviation is deceptive in that most of the deviations comes from a few large lines. However on a line-by-line basis the Rouillé et al data are slightly better than the calculations of Ref. 13.

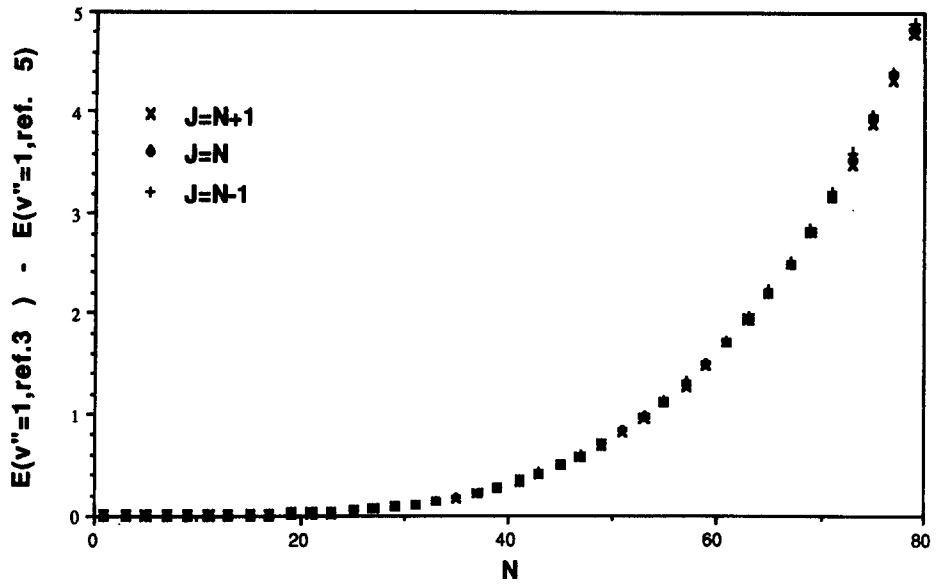

Fig. 5. Energy difference in cm^{-1} between the formalism of Rouillé et al[21] and Greenbaum[13] vs N for the $v'' = 1$ states of $X^3\Sigma_g^-$ of $^{16}O_2$.

0.145×10^{-26} esu cm^2, not in agreement with the quadrupole moment derived from far-I.R. PIA spectra[25] (see previous section). This is under investigation. Comparing the 1996 and 1992 values for the intensities we find an average ratio of 1.0027, with some ratios between 0.740 and 1.31. These large ratios occur for 33 out of the 146 lines and occur only for forbidden (weaker) lines, with $\Delta N \neq \Delta J$ and at low J.

The 1996 calculations for this band are not filtered through a cutoff procedure and many of the lines will have very small intensities. (In fact, one zero intensity magnetic dipole and electric quadrupole transition have been retained in the data for theoretical considerations; it helps to see the effects of assumed parameters on these lines.) There are 254 md transitions and 183 eq transitions retained for this band.

5.1.3. The $X^3\Sigma_g^-$ $(v = 1) \leftarrow X^3\Sigma_g^-$ $(v = 1)$ *band.* As discussed above, the energy differences from the previous calculations and the formulation of Rouillé et al[21] for the $v = 1$ level approach 5 cm^{-1} at N = 80. The maximum energy difference in the lines in the 1996 data is 0.750 cm^{-1} and the average difference is -0.0953 cm^{-1}. The maximum difference in line positions is 0.0457 cm^{-1} with the average difference being -0.00280 cm^{-1}. The intensity ratios are between 0.994 and 0.988 with an average ratio of 0.990. Most of this difference comes from using an improved partition sum in the calculations.

5.1.4. The $a^1\Delta_g$ $(v = 0) \leftarrow X^3\Sigma_g^-$ $(v = 0)$ *band.* There are wavenumber differences which arise from a change in the energy formulation of $X^3\Sigma_g^-$ $(v = 0)$ to that of Rouillé et al[21] and for $a^1\Delta_g$ $(v = 0)$ to that of Scalabrin et al[29] with the constants of Hillig *et al.*[30] The maximum difference is 0.0160 cm^{-1} at $N'' = 37$ and the average difference is -0.00234 cm^{-1}.

The line intensities for this band are calculated using Eq. (11). There are three measurements of the band intensity in the literature (scaled to 296 K) which differ by a factor of about 4.5. The measurement of Badger et al[31] gives $S_{00} = 3.6 \times 10^{-24}$ cm^{-1}/(molecule cm^{-2}). The measurement of Lin et al[32] is $S_{00} = 9.4 \times 10^{-24}$ cm^{-1}/(molecule cm^{-2}), and Hsu et al[33] report a value of $S_{00} = 2.1 \times 10^{-24}$ cm^{-1}/(molecule cm^{-2}). From these values the authors determine the Einstein-A coefficient. Unfortunately, some of the authors have used incorrect statistical degeneracy factors, d_ℓ/d_u; Badger et al[31] used 3/2 whereas Lin et al[32] and Hsu et al[33] use 3/1. It was demonstrated above that in Eq. (11) $d_\ell = 3$ and $d_u = 2$. Thus, application of Eq. (11) (or Eq. (10)) will only generate consistent line intensities if the statistical degeneracy factors and the derived Einstein-A coefficient are from the same author. Because of the large discrepancy between the measured band intensities, we sought to determine the band intensity from another source. We have

Table 4. Measured intensities (Brault and Brown[34]) of the $a^1\Delta_g$ ($v = 0$)← $X^3\Sigma_g^-$ ($v = 0$) band, final HITRAN96 values, ratios, and final average ratio

Line†	Brault and Brown[34] [cm^{-1}/(molecule cm^{-2})]	HITRAN96 [cm^{-1}/(molecule cm^{-2})]	Ratio
O23P22	2.44E-27	2.65E-27	0.92145
O10P18	6.47E-27	6.87E-27	0.94205
P23P23	5.67E-27	5.56E-27	1.019234
P23Q22	6.99E-27	6.12E-27	1.142344
O13P12	1.67E-26	1.62E-26	1.030864
P21P21	9.10E-27	9.36E-27	0.972118
P21Q20	1.02E-26	1.04E-26	0.982659
P19P19	1.43E-26	1.47E-26	0.970808
O11P10	1.90E-26	1.78E-26	1.065022
P19Q18	1.70E-26	1.65E-26	1.030303
P17P17	2.06E-26	2.16E-26	0.954588
O9P8	1.75E-26	1.72E-26	1.018034
P15P15	2.75E-26	2.93E-26	0.937287
P15Q14	3.45E-26	3.38E-26	1.019805
		Average	1.000469

†Branch symbol for ΔN, N''; branch symbol for ΔJ, J''.

obtained unpublished line intensity measurements[34] of 14 transitions in the $a^1\Delta_g$ ($v = 0$)← $X^3\Sigma_g^-$ ($v = 0$) band that were mentioned in the work of Wallace and Livingston.[35] Using our O_2 program, the Einstein-A coefficient used to calculate the line intensities was scaled to match the measurements of Ref. 34. The results are in Table 4. This fit gives a band intensity of $S_{00} = 3.69 \times 10^{-24}$ cm^{-1}/(molecule cm^{-2}) which is close to the Badger et al[31] value. The Einstein-A coefficients, the band intensities, and the statistical degeneracy factors as related by Eq. (10) are listed in Table 5. The calculation of the line intensities for the 1996 database used the Einstein-A coefficient $A = 2.59 \times 10^{-4}$ sec^{-1} with statistical degeneracy factors of $d_\ell = 3$ and $d_u = 2$. The resulting line intensities are larger than HITRAN92 by roughly a factor of 2; this is due to incorrect inversion from Badger et al's A to S used in previous versions of HITRAN. Suspicion of such missing factors of 2, and concerns about the interpretation of upper atmosphere emissions, such as inferring ozone from SME (Solar Mesophere Explorer via the $a^1\Delta_g$ 1.27 μm airglow) were expressed by Mlynczak and Nesbitt[36] (who conjectured a significant change in A from one of the reported S values in Table 5 (Hsu et al[33])) and by Pendelton et al.[37] Recent observations in the mesosphere[38] confirm the Badger et al[31] value of the Einstein-A coefficient. Moreover, new line intensity measurements made at National Institute for Standards and Technology[39] and at Rutherford Appleton Laboratory[40] are roughly 15% larger than the HITRAN96 values. Preliminary comparisons indicate agreement between these two new independent high-resolution studies. When completed, these data will be incorporated into the next edition of HITRAN.

5.1.5. The $a^1\Delta_g$ ($v = 1$)← $X^3\Sigma_g^-$ ($v = 0$) band. The molecular constants for the $a^1\Delta_g$ ($v = 1$) state are from Brault.[41] Line positions have changed 0.001302 cm^{-1} on average.

The Einstein-A coefficient used is 1/200 of the value of the $a^1\Delta_g$ ($v = 0$)←($v = 0$) band,[42] hence the line intensities are increased by 1.46 on average. Unfortunately, to our knowledge, no other observations of this band are available to perform a proper test of this adopted ratio. The line positions and energies have only changed by -0.000273 cm^{-1} and 0.000388 cm^{-1} on average.

5.1.6. The $a^1\Delta_g$ ($v = 0$)← $X^3\Sigma_g^-$ ($v = 1$) band. The wavenumbers have changed due to the reformulation of the energy expressions for both the upper and lower states,[21,29] resulting in an average change of 0.0157 cm^{-1}. The line intensities are calculated using one tenth of the Einstein-A coefficient of the $a^1\Delta_g$ ($v = 0$)← $X^3\Sigma_g^-$ ($v = 0$) band[42] and are larger than previous HITRAN

Table 5. Measured band intensities, derived Einstein-A coefficients, and statistical degeneracy factors for the $a^1\Delta_g(v = 0)$←$X^3\Sigma_g^-(v = 0)$ band

Reference	S_{00} [cm^{-1}/(molecule cm^{-2})]	$A_{v'A'_1 \to v''A''_1}$ (sec^{-1})	d_ℓ/d_u
Badger et al[31]	3.66×10^{-24}	2.58×10^{-4}	3/2
Lin et al[32]	9.4×10^{-24}	1.3×10^{-4}	3/1
Hsu et al[33]	2.1×10^{-24}	2.9×10^{-4}	3/1
Fit of data[34]†	3.69×10^{-24}	2.59×10^{-4}	3/2

†Adopted for HITRAN96.

databases[5] by an average of 2.04. The same comment as above applies to the adopted ratio used for this band.

5.1.7. The $b^1\Sigma_g^+$ $(v = 0) \leftarrow X^3\Sigma_g^-$ $(v = 0)$ *band (A-band).* The constants for the $b^1\Sigma_g^+$ $(v = 0)$ state are from Zare et al[43] and those for the $X^3\Sigma_g^-$ $(v = 0)$ state are from Rouillé et al.[21] The wavenumbers differ by -0.00127 cm^{-1} on average, with the maximum difference being 0.00383 cm^{-1}. The average energy difference is 0.00134 cm^{-1}. Intensity ratios vary from 0.825 to 0.877, with the average ratio being 0.862. The Einstein-A coefficient has been changed from the value of Miller et al[44] 0.077 sec^{-1} to the newer value of 0.0887 from Ritter and Wilkerson.[18]

5.1.8. The $b^1\Sigma_g^+(v = 1) \leftarrow X^3\Sigma_g^-$ $(v = 0)$ *band (B-band).* The constants for the $X^3\Sigma_g^-$ $(v = 1)$ state are from Zare et al[43] and those for the $X^3\Sigma_g^-$ $(v = 0)$ state are from Rouillé et al.[21] The wavenumber and energies arise from changes made to the ground state energies. The maximum wavenumber and energy differences are 0.00383 cm^{-1} and 0.00370 cm^{-1}, respectively. The intensity ratios range from 0.782 to 0.822 with an average of 0.811. The value of the Einstein-A coefficient is from Giver et al,[19] $A(1\text{–}0) = 0.00724$ sec^{-1}, but was incorrectly used in the previous program where it was set to $A(1\text{–}0) = 0.00591$ sec^{-1}.

5.1.9. The $b^1\Sigma_g^+$ $(v = 2) \leftarrow X^3\Sigma_g^-$ $(v = 0)$ *band (γ-band).* The constants for the $b^1\Sigma_g^+$ $(v = 2)$ state are also from Zare et al[43] and those for the $X^3\Sigma_g^-$ $(v = 0)$ state are from Rouillé et al.[21] The average wavenumber and energy differences are 0.00694 cm^{-1} and 0.00104 cm^{-1}. The intensity ratios range from 1.22 to 1.27. The Einstein-A coefficient of Mélières et al[20] is now used, $A(2\text{–}0) = 2.69 \times 10^{-4}$ sec^{-1}. Compared with the older value from Miller et al[45] of $A(2\text{–}0) = 3.24 \times 10^{-4}$ sec^{-1} (which was incorrectly used as $A(2\text{–}0) = 2.2 \times 10^{-4}$ sec^{-1} in the HITRAN82[5] calculations) an average ratio of 0.813 is obtained.

5.1.10. The $b^1\Sigma_g^+$ $(v = 1) \leftarrow X^3\Sigma_g^-$ $(v = 1)$ *band.* The molecular constants used in the calculation of energies are from Zare et al[43] for the $b^1\Sigma_g^+$ $(v = 1)$ state and from Rouillé et al[21] for the $X^3\Sigma_g^-$ $(v = 1)$ state. The line positions show a maximum difference of 0.0857 cm^{-1} with an average of 0.0207 cm^{-1}. The difference is due to the change in the ground state energies. The Einstein-A coefficient is from Giver *et al.*[19] The intensity ratios range from 0.962 to 0.999. These changes are due to the correct partition sums and removal of some approximations in the formulas.

5.1.11. The $b^1\Sigma_g^+$ $(v = 0) \leftarrow X^3\Sigma_g^-$ $(v = 1)$ *band.* The molecular constants are from Zare et al[43] for the $b^1\Sigma_g^+$ $(v = 0)$ state and from Rouillé et al[21] for the $X^3\Sigma_g^-$ $(v = 1)$ state. The changes in the line positions are from the new lower state energies. The maximum value is 0.0333 cm^{-1} and the average is 0.00935 cm^{-1}. The Einstein-A coefficient is from Galkin.[46] The resulting intensity ratios range from 0.968 to 1.00.

5.2. The $^{16}O^{18}O$ *species*

5.2.1. The $X^3\Sigma_g^-$ $(v = 0) \leftarrow X^3\Sigma_g^-$ $(v = 0)$ *band.* The present calculations use the improved molecular constants of Mizushima and Yamamoto.[47] The resulting energies differ from previous calculations by 0.0174 cm^{-1} on average with a maximum difference of 0.136 cm^{-1} at $N = 53$. The average difference in line position is 0.00112 cm^{-1} with the largest difference being 0.00962 cm^{-1}. The line intensities differ only by a few percent maximum which is attributed to the improved partition sums.

5.2.2. The $a^1\Delta_g$ $(v = 0) \leftarrow X^3\Sigma_g^-$ $(v = 0)$ *band.* There is a slight change in some of the wavenumbers due to the change in energy formulation for the $X^3\Sigma_g^-$ $(v = 0)$ state [21]. This gives rise to a maximum difference of 0.00580 cm^{-1} and an average difference of -0.00127 cm^{-1}. Intensity ratios are ≈ 0.5 as expected and 49 of the previous lines do not make the intensity cut off.

5.2.3. The $b^1\Sigma_g^+$ $(v = 0) \leftarrow X^3\Sigma_g^-$ $(v = 0)$ *band.* The energies of the $X^3\Sigma_g^-$ $(v = 0)$ state are calculated using the constants of Mizushima and Yamamoto.[47] The constants for the $b^1\Sigma_g^+$ $(v = 0)$ state are from Babcock and Herzberg.[48] Wavenumber differences of 0.0242 cm^{-1} at $N'' = 34$ are observed with an average difference of -0.00577 cm^{-1}. The average intensity ratio is 0.882 due mostly to the change in partition functions.

5.2.4. The $b^1\Sigma_g^+$ $(v = 1) \leftarrow X^3\Sigma_g^-$ $(v = 0)$ *band.* The constants for the $b^1\Sigma_g^+$ $(v = 1)$ state are from Benedict.[49] Those for the $X^3\Sigma_g^-$ $(v = 0)$ state are from Mizushima and Yamamoto.[47] The maximum wavenumber difference is 0.0107 cm^{-1}. This difference is due to the change in the lower state energies. The Einstein-A coefficient is from Giver et al.[19] The average ratio of the intensities 0.830.

5.2.5. The $b^1\Sigma_g^+$ $(v = 2) \leftarrow X^3\Sigma_g^-$ $(v = 0)$ *band.* The constants for the $b^1\Sigma_g^+$ $(v = 2)$ state are from Zare *et al.*[43] Those for the $X^3\Sigma_g^-$ $(v = 0)$ state are from Mizushima and Yamamoto.[47] The maximum wavenumber difference is 0.150 cm^{-1} and the average intensity ratio is 0.837. Caution must be used in interpreting these numbers since the comparison is based on only 3 lines.

5.3. The $^{16}O^{17}O$ *species*

5.3.1. The $X^3\Sigma_g^-$ $(v = 0) \leftarrow X^3\Sigma_g^-$ $(v = 0)$ *band.* The data for this band are taken from the Jet Propulsion Laboratory catalogue.[50] There are 10 787 lines in the JPL file. The data were filtered through the wavenumber dependent cutoff resulting in 2601 lines from 0.000012 cm^{-1} to 186.15 cm^{-1} in the final file. Note the isotopic abundance factor was inadvertently omitted from the 1996 HITRAN database. Thus, the ratio of the line intensity (S92/S96) is 0.000750 on average. In order to properly use the intensities for these data, they should be multiplied by $I_a = 0.000742235$. The line positions and lower state energies have only changed slightly, 0.000041 cm^{-1} and -0.000352 cm^{-1} average difference respectively.

5.3.2. The $b^1\Sigma_g^+$ $(v = 1) \leftarrow X^3\Sigma_g^-$ $(v = 0)$ *band.* These data are from Benedict and Brault[51] and have not changed from the 1982 HITRAN database.

6. OTHER CHANGES

We have added reference and error codes to the line parameter database. The error code (see HITRAN96 manual[52]) for the halfwidths is set to 4. The error code for the line positions of $X^3\Sigma_g^- \leftarrow X^3\Sigma_g^-$ electronic band is set to 4 and all other error codes are not utilized on the database (i.e. set to 0). We have also labeled the electric quadrupole and magnetic dipole transitions by the lower case letters *q* and *d*, respectively, in the sym field of the rotational quantum number character string, i.e., Br, F'',__;Br, N'', Br, J'', ____, Sym.

These data are available in the 1996 HITRAN database.[52]

7. O_2 CONTINUUM ABSORPTION

It is known that the $O_2 X^3\Sigma_g^-(v'') - a^1\Delta_g(v')$ absorption bands exhibit both discrete (rotational) line structure and pressure-induced continuous absorption.[31] The most important bands are the $v'' = 0$, $v' = 0$ at 1.27 μm (7882 cm^{-1}), $v'' = 0$, $v' = 1$ at 1.06 μm (9366 cm^{-1}), and $v'' = 1$, $v' = 0$ at 1.6 μm (6326 cm^{-1}). While the rotational lines of the (0–1) band are weaker than those of (0–0) band, and those of (1–0) band are weaker than the (0–1) band, the continuum absorptions are of more similar intensity.

During the update of the (0–0) band line parameters, theoretical calculations were compared with absolute atmospheric transmittance obtained with the University of Denver Absolute Solar Transmittance Interferometer (ASTI).[53] The results show good agreement of the line structure but a clear indication of the underlying continuum (not modeled), with the *P*, *R* (no *Q*) shape of the envelope under the absorption lines. The continuum is clearer at the higher spectral resolution (≥ 0.5 cm OPD).

More recent ASTI data in the 9400 cm^{-1} and 6400 cm^{-1} regions also show a strong continuum, similar to that described above. It is thus proposed that this is due to the pressure-induced absorption of the $v'' = 0$, $v' = 1$ and $v'' = 1$, $v' = 0$ bands respectively.[54] Laboratory data[55] are consistent with these conclusions, but indicate no pressure-induced absorptions under the $X^3\Sigma_g^-(v'') - b^1\Sigma_g^+(v')$ bands. The pressure-induced absorption in the $X^3\Sigma_g^-(v'' = 0) - X^3\Sigma_g^-(v' = 1)$ has been well documented in previous publications.[25, 56, 57]

In the HITRAN database we have included the individual line parameters of these bands, but no cross-sections are provided for the continuum. These cross-sections will be forthcoming on the next version of the HITRAN database.

Acknowledgements—The authors are pleased to acknowledge support of this research by the Air Force Office of Scientific Research Task 2310G1. The research at the University of Denver was also supported by the National Science Foundation, Atmospheric Chemistry Division.

REFERENCES

1. Thomas, R. J., Barth, C. B., Rusch, D. W. and Sanders, R. W., *J. Geophys. Res.*, 1984, **89,** 9569.
2. Mlynczak, M. G., Solomon, S. and Zarus, D. S., *J. Geophys. Res.*, 1993, **98,** 18,639.
3. Rothman, L. S. and Goldman, A., *Appl. Opt.*, 1981, **20,** 2182.
4. Rothman, L. S., Gamache, R. R., Goldman, A., Flaud, J.-M., Tipping, R. H., Rinsland, C. P., Smith, M. A. H., Toth, R. A., Brown, L. R., Devi, V. M. and Benner, D. C., *J. Quant. Spectrosc. Radiat. Transfer*, 1992, **48,** 469.
5. Rothman, L. S., Gamache, R. R., Barbe, A., Goldman, A., Gillis, J. R., Brown, L. R., Toth, R. A., Flaud, J.-M. and Camy-Peyret, C., *Appl. Opt.*, 1983, **22,** 2247.
6. Cohen, E. R. and Taylor, B. N., *Phys. Today*, 1995, August, BG9–BG13.
7. Herzberg, G., *Molecular Spectra and Molecular Structure I. Spectra of Diatomic Molecules*, 2nd edn. Van Nostrand, New York, 1966.
8. Herzberg, G., *Molecular Spectra and Molecular Structure II. Infrared and Raman Spectra of Polyatomic Molecules*. Van Nostrand, New York, 1960.
9. Tinkham, M. and Strandberg, M. W. P., *Phys. Rev.*, 1955, **97,** 937.
10. Steinbach, W. and Gordy, W., *Phys. Rev. A*, 1973, **8,** 1753.
11. Steinbach, W. and Gordy, W., *Phys. Rev. A*, 1975, **11,** 729.
12. Steinbach, W. R., Millimeter and submillimeter wave spectra of the oxygen isotopes: $^{16}O_2$, $^{18}O_2$, and $^{16}O^{18}O$. Ph.D. Thesis, Department of Physics, Duke University, 1974.
13. Greenbaum, M., The calculation of millimeter and submillimeter wave absorption line parameters for the molecular oxygen isotopes: $^{16}O_2$, $^{16}O^{18}O$, $^{18}O_2$. Riverside Research Institute Technical Report T-1/306-3-14,80, West End Avenue, New York, NY 10023, 1975.
14. Penner, S. S., *Quantitative Molecular Spectroscopy and Gas Emissivities*. Addison-Wesley, Reading, MA, 1959.
15. Gamache, R. R. and Rothman, L. S., *J. Quant. Spectrosc. Radiat. Transfer*, 1992, **48,** 519.
16. Krupenie, P. H., *J. Phys. Chem. Ref. Data*, 1972, **2,** 423.
17. Gamache, R. R., Hawkins, R. L. and Rothman, L. S., *J. Mol. Spectrosc.*, 1990, **142,** 205.
18. Ritter, K. J. and Wilkerson, T. D., *J. Mol. Spectrosc.*, 1987, **121,** 1.
19. Giver, L. P., Boese, R. W. and Miller, J. H., *J. Quant. Spectrosc. Radiat. Transfer*, 1974, **14,** 793.
20. Mélières, M. A., Chenevier, M. and Stoeckel, F., *J. Quant. Spectrosc. Radiat. Transfer*, 1985, **33,** 337.
21. Rouillé, G., Millot, G., Saint-Loup, R. and Berger, H., *J. Mol. Spectrosc.*, 1992, **154,** 372.
22. Loete, M. and Berger, H., *J. Mol. Spectrosc.*, 1977, **68,** 317.
23. Welch, W. M. and Mizushima, M., *Phys. Rev. A*, 1972, **5,** 2692.
24. Zink, L. R. and Mizushima, M., *J. Mol. Spectrosc.*, 1987, **125,** 154.
25. Cohen, E. R. and Birnbaum, G., *J. Chem. Phys.*, 1977, **66,** 2443.
26. Benedict, W. S. and Kaplan, L. D., *J. Quant. Spectrosc. Radiat. Transfer*, 1964, **4,** 453.
27. Goldman, A., Rinsland, C. P., Canova, B., Zander, R. and Dang-Nhu, M., *J. Quant. Spectrosc. Radiat. Transfer*, 1995, **54,** 757.
28. Reid, J., Sinclair, R. L., Robinson, A. M. and McKellar, A. R. W., *Phys. Rev. A*, 1981, **24,** 1944.
29. Scalabrin, T., Saykally, R. J., Evenson, K. M., Radford, H. E. and Mizushima, M., *J. Mol. Spectrosc.*, 1981, **89,** 344.
30. Hillig II, K. W., Chiu, C. C. W., Read, W. G. and Cohen, E. A., *J. Mol. Spectrosc.*, 1985, **109,** 205.
31. Badger, R. M., Wright, A. C. and Whitlock, R. F., *J. Chem. Phys.*, 1965, **43,** 4345.
32. Lin, L.-B., Lee, Y.-P. and Ogilvie, J. F., *J. Quant. Spectrosc. Radiat. Transfer*, 1988, **39,** 375.
33. Hsu, Y. T., Lee, Y. P. and Ogilvie, J. F., *J. Quant. Spectrosc. Radiat. Transfer*, 1992, **48A,** 1227.
34. Brault, J. and Brown, M. M., Unpublished results.
35. Wallace, L. and Livingston, W., *J. Geophys. Res.*, 1990, **95,** 9823.
36. Mlynczak, M. G. and Nesbitt, D. J., *Geophys. Res. Lett.*, 1995, **22,** 1381.
37. Pendelton, W. R. jr, Baker, D. J., Reese, R. J. and O'Neil, R. R., *Geophys. Res. Lett.*, 1996, **23,** 1013.
38. Sandor, B. J., Clancy, R. T., Rusch, D. W., Randall, C. E., Eckman, R. S., Siskind, D. S. and Muhleman, D. O., *J. Geophys. Res.*, 1997, **102,** 9013.
39. Lafferty, W., National Institute of Standards and Technology, Private communication, 1996.
40. Newnham, D. A., Ballard, J. and Page, M. S., Visible absorption spectroscopy of molecular oxygen, Paper A7, Atmospheric Spectroscopy Applications Workshop, 4–6 September 1996. Reims, France.
41. Brault, J., Private communication, 1982.
42. Jones, A. V. and Harrison, A. H., *J. Atmos. Terr. Phys.*, 1958, **13,** 45.
43. Zare, R. N., Schmeltekopf, A. L., Harrop, W. J. and Albritton, D. L., *J. Mol. Spectrosc.*, 1973, **46,** 37.
44. Miller, J. H., Boese, R. W. and Giver, L. P., *J. Quant. Spectrosc. Radiat. Transfer*, 1969, **9,** 1507.
45. Miller, J. H., Giver, L. P. and Boese, R. W., *J. Quant. Spectrosc. Radiat. Transfer*, 1976, **16,** 595.
46. Galkin, V. D., *Opt. Spectrosc. (USSR)*, 1979, **47,** 151.
47. Mizushima, M. and Yamamoto, S., *J. Mol. Spectrosc.*, 1991, **148,** 447.
48. Babcock, H. and Herzberg, L., *Astrophys. J.*, 1948, **108,** 167.
49. Benedict, W. S., Private communication, 1982.
50. Poynter, R. L., Pickett, H. M., Cohen, E. A., Delitsky, M. L., Pearson, J. C. and Müller, H. S. P.,

Submillimeter, millimeter, and microwave spectral line catalogue, JPL publication 80-23, Revision 4, 10 March 1996.
51. Benedict, W. S. and Brault, J., Private communication, 1982.
52. Rothman, L. S., Rinsland, C. P., Goldman, A., Massie, S. T., Edwards. D. P., Flaud, J.-M., Perrin, A., Dana, V., Mandin, J.-Y., Schroeder, J., McCann, A., Gamache, R. R., Wattson, R. B., Yoshino, K., Chance, K. V., Jucks, K. W., Brown L. R., Nemtchinov, V., and Varanasi P., in preparation.
53. Goldman, A., The role of laboratory spectroscopy in the analysis of atmospheric spectra, Atmospheric Spectroscopy Applications (ASA) Colloquium, Reims, France, 4–6 September 1996.
54. Goldman, A., Extended quantitative spectroscopy for analysis of atmospheric infrared spectra, Fourier Transform Spectroscopy OSA—Topical Meeting, Santa Fe, New Mexico, 10–12 February 1997.
55. Greenblat, G. D., Orlando, J. J., Burkholder, J. B. and Ravishankara, A. R., *J. Geophys. Res.*, 1990, **95,** 18,577.
56. Orlando, J. J., Tyndall, G. S., Nickerson, K. E. and Calvert, J. G., *J. Geophys. Res.*, 1991, **96,** 20,755.
57. Rinsland, C. P., Smith, M. A. H., Seals, R. K. jr, Goldman, A., Murcray, F. J., Murcray, D. G., Larsen, J. C. and Rarig, P. L., *J. Geophys. Res.*, 1982, **87,** 3119.